Iraqi Journal of Science, 2025, Vol. 66, No. 10, pp: 4344 – 4361
DOI: 10.24996/ijs.2025.66.10.25

ISSN: 0067-2904

# Gold Mineralisation in Metamorphic Rocks on Buru Island, Indonesia: Rock Facies, Geochemistry, Alterations, Mineralisation, and Types of Ore Deposits

**Alam Budiman Thamsi[1*], Muhamad Hardin Wakila[1], Nurliah Jafar[1], Lamatinulu[2], Irzal Nur[3], Rohaya Langkoke[4], Ilham Alimuddin[4], Muhammad Aswadi[5], Ahmad Jeli[6]**

[1]*Department of Mining Engineering, Faculty of Industrial Technology, Universitas Muslim Indonesia, Indonesia*

[2] *Department of Studies Industrial Engineering, Faculty of Industrial Technology, Universitas Muslim Indonesia, Indonesia*

[3] *Department of Mining Engineering, Faculty of Engineering, Universitas Hasanuddin, Indonesia*

[4]*Department of Geological Engineering, Faculty of Engineering, Universitas Hasanuddin, Indonesia*

[5]*Department of Geological Engineering, Faculty of Engineering, Universitas Tadulako, Indonesia*

[6]*Department of Mining Engineering, Faculty of Engineering, Colorado School of Mines, USA*

Received: 14/2/2025 Accepted: 9/7/2025 Published: 30/10/2025

**Abstract**

Indonesia is a country rich in natural resources, one of which is gold deposits scattered across several locations, including the islands of Sumatra, Java, Sulawesi, Maluku, Nusa Tenggara and Papua. This study aims to (1) determine the type of alteration contained in the research area based on the altered mineral set resulting from the alteration process and the characteristics of gold deposits in metamorphic rocks in the study area, (2) determine the mineralisation characteristics of gold deposits by conducting geochemical analysis, (3) determine the type of metamorphic facies in host-rocks Gold deposits in the research area, (4) explain how the distribution of gold content from the results of geochemical analysis, (5) explain the genetic characteristics of gold deposits in the study area based on geochemical analysis and petrographic analysis. This study involved a field survey and random rock sampling at Mount Botak, Buru Regency, Maluku Province, Indonesia. Rock samples were analysed by petrographic analysis, XRD (X-ray Diffraction) analysis, XRF (X-ray fluorescence) analysis, ICP-OES (inductively coupled plasma-optical emission spectrometry) analysis, and AAS (atomic absorption spectrometry) analysis. The study results indicate that the host rock of gold deposits on Buru Island is a metamorphic rock formed by greenschist facies. The types of alterations are silicic, sericitization, argilic, and chloritization. The mineralisation is generally in quartz veins with a crustiform texture and a slight vein stockwork. Au levels ranged from 0.23 to 5.9 g/ton, which was not accompanied by Ag enrichment. Based on the analysis of gold deposits in the research area, it is an orogenic-type of deposit formed in a mesozonal environment, typically at a depth of 5-10 km. The implications of the research results can be applied to gold exploration purposes in Indonesia, particularly for gold deposits that have metamorphic host rocks.

**Keywords:** Orogenic Gold Deposits, Geology, Au-Sb-As, Mount Botak.

*Email: alambudiman.thamsi@umi.ac.id

## 1. Introduction

Gold mining activities in Indonesia are mostly carried out on types of host-volcanic hydrothermal deposits, which include epithermal types, such as Pongkor in West Java [1], [2], [3], Gosowong on Halmahera Island [4] types of skarn, e.g., Ertsberg, Wild Cats, Deep Ore Zone (DOZ) in Papua [5], [6], [7] types of porphyry, for example, Batu Hijau on Sumbawa Island [8], [9] and organic gold deposits in the areas of Bombana, Awak Mas, Rampi, and Buru Island [10]. Gold exploration activities are primarily focused along the volcanic belt and begin to shift along metamorphic paths. These gold deposits are known as organic gold deposits. In the latest development, residents on Buru Island found gold nuggets in Mount Botak and the Gogorea area, Maluku Province, Indonesia [11]. Several previous researchers have reported the prospect of primary gold mineralisation in metamorphic rock-hosted gold mineralisation on Buru Island [11], [12]. The prospect of mineralisation is relatively new since the rush (gold mining hunt) occurred when people mined gold in several locations on Buru Island, especially in Mount Botak and Gogorea, Buru Regency.

Several studies have been conducted in the gold deposits of metamorphic host-rocks located in several regions in Indonesia, including Mas, Rampi, Palopo, Bombana, and Buru [13], [14], [15], [16], [17], [18], [19], [20]. Previous researchers have investigated the characteristics of gold deposits in geological settings, mineralisation, geochemistry, alteration, fluid inclusion, and deposit genetics. In the Buru Island area, studies have reported, among other things, the discovery of segmented, sigmoidal, discontinuous, and quartz veins that are parallel to the foliation field of the host metamorphic rocks (especially mica schists). The quartz vein mineralisation zone is about 1 km wide by about 100 m, overprinted by the argillic alteration zone, and strongly controlled by north-south and northeast-southwest directional structures. Quartz veins containing gold are generally textured, colloform, banded, sulfide banding, brecciated, and slightly bladed-like. The alterations are propylitic (chlorite, calcite, sericite), argilic, and carbonated. The ore mineralisation consists of pyrite, native gold, pyrrhotite, and arsenopyrite, as well as a small amount of cinnabar, stibnite, chalcopyrite, galena, and sphalerite. The gold content is 1-3 grams per ton [11], [12].

No research has examined the tectonics, host-rock facies, and genesis of gold deposits in the research area. This research gap needs to be addressed to provide new insights into the formation of gold deposits. Recently, research on primary gold deposits in Indonesia has focused more on gold deposits in metamorphic rocks [11]. One of them is Buru Island, an area with gold potential, which is evident from the people's mining activities that have been carried out there to date. Scientific research on the Buru Island area, which specialises in the potential of mineral resources, such as alteration and mineralisation research, can help the local government obtain information about the characteristics of gold deposits in the area.

In connection with the above, the author conducted a study entitled Gold Mineralisation in Metamorphic Rocks on Buru Island, Indonesia: Rock facies, geochemistry, alteration, mineralisation, and types of ore deposits. This study aims to determine the type of alteration contained in the research area based on the altered mineral set resulting from the alteration process and the characteristics of gold deposits in metamorphic rocks in the study area, determine the mineralisation characteristics of gold deposits by conducting geochemical analysis, determine the type of metamorphic facies in host-rocks gold deposits in the research area, explain how the distribution of gold content from the results of geochemical analysis, describe the genetic characteristics of gold deposits in the study area based on geochemical analysis and petrographic analysis.

The regional geology of Buru Island consists of 18 rock formations, namely the Wahua Complex (Pzw), the Rana Complex (Pzr), the Ghegan Formation (Trg), the Dalan Formation (Trd), the Mefa Formation (Jm), Diabas (JKd), the Kuma Formation (MTk), the Waeken Formation (Tomw), the Wakatin Formation (Tmw), the Hutong Formation (Tmh), the Ftau Formation (Tmfv), the Andesite (Tpa), the Ambalau Volcanic Rock (Tpav), the Leko Formation (Tpl), the Reef Limestone (Ql), the Lake Sediments (Qd), and Alluvial (Qa). The Wahua Complex (Pzw) consists of schist, filit, meta-arkosic sandstone, quartzite, and marble of Palaeozoic age. The Rana Complex (Pzr) consists of phyllite, rocks, meta-arkose, meta-greywacke, and marble of the Palaeozoic age. The Ghegan Formation (Trg) consists of dolomitic limestone, calcarenite, shale, and marl of Mesozoic age. The Dalan Formation (Trd) consists of sandstone, shale, siltstone, and conglomerate of Mesozoic age. The Mefa Formation (Jm) consists of basal lava and tufa of the Jurassic age. Diabase (JKd) is of Jurassic to Cretaceous age. The Kuma Formation (MTk) consists of Calcilutite, Cherty lutite, chert, marl, and conglomerate of Mesozoic to Tertiary age. The Waeken (Tomw) formation consists of napal, sand, and calcilutite of Tertiary age, Oligocene to Miocene. The Wakatin Formation (Tmw) consists of coral limestone of the Miocene age. Hotong Formation (Tmh) consists of sandstone, clay shale, siltstone, limestone, and conglomerate of tertiary Miocene age. The Ftau (Tmfv) formation consists of andesitic lava, volcanic breccia, and Miocene-aged tuff. Andesite (Tpa) of Miocene age. Ambalu volcanic rocks (Tpav) consist of andesitic lava and pyroclastics of the Pliocene age. The Leko formation (Tpl) comprises Pliocene age conglomerate, sandstone, and limestone. Reef limestone, gravel, sand, peat-silt, and quaternary-age mud [21].

The geological structure of Buru Island is grouped into several faults. A fault mirror, burly lithological offset, gain, and triangular facet were found. The research location is included in the Wahlua complex (Figure 1). The schist rocks in the area are of Palaeozoic age. Metamorphic rocks on Buru Island are reportedly derived from flysch sediments [22]. There is a fault in the southeastern part of the research site, which is usually associated with the presence of orogenic gold deposits [11], [23], [24], [25], [26].

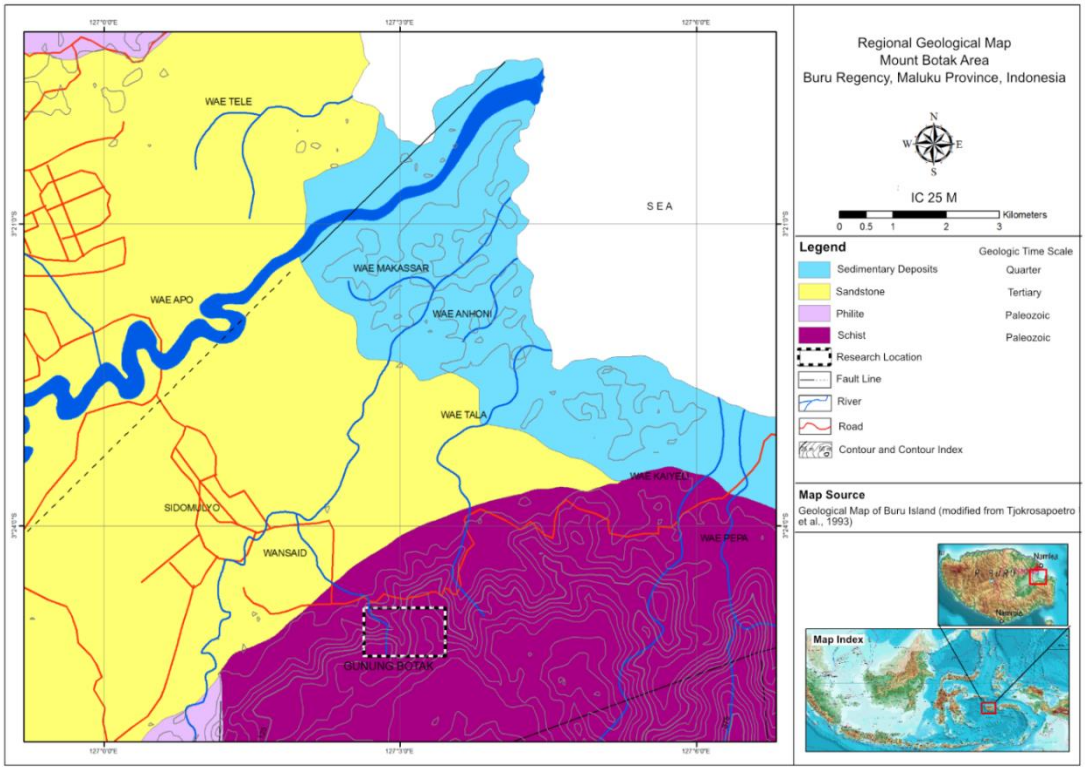


**Figure 1:** Geological map of the research area (modified after Tjokrosapoetra [26])

## 2. Materials and Methods

This research activity was conducted on Buru Island, Maluku Province, located on Mount Botak. Mount Botak is geographically situated at 127°2'15"E—127°3'45"E and 3°23'05"LS-3°25'15" E. The tools and materials used in this study include a geological compass, a geological hammer, a topographic map, a geological map, a sample bag, a Loupe 30X, a Garmin 76CSX Global Positioning System (GPS) device, a Camera, a Solution, a field book, and QGIS Software. Sampling was conducted at the study site. Rock samples were taken directly in the field at random at each outcrop point of the altered rocks and host rocks of gold deposits found in the field. Each outcrop is sampled, plotted, photographed and labelled. Primary data in the field was obtained from observations in the field; this stage consisted of observation of altered outcrops, observation of hydrothermal changes, observation of mineralisation changes, taking samples of altered rocks, taking samples of rocks (host-rock), field documentation, conducting laboratory analyses of petrography, mineralisation, and chemistry.

Petrography analysis aims to determine the type of host rock associated with gold deposits found on Buru Island in the Mount Botak area. In the sample, a thin section will be made parallel to the foliation and perpendicular to it. This aims to determine the influence of structure on the presence of gold deposits. This analysis also intends to determine the samples' sets and types of altered and mineralised minerals based on their optical properties. In addition, petrographic analysis is also used to analyse certain alteration textures, such as replacement or fig-filling textures. This information is indispensable for conducting mineral paragenesis studies. There are four thin-section samples.

Several geochemical analyses are used in this analysis, namely X-ray Diffraction (XRD), X-ray fluorescence (XRF) and inductively coupled plasma–optical emission spectrometry (ICP-OES) [27], and atomic absorption spectrometry (AAS).

Observation of minerals with a microscope is sometimes constrained because the material is soft, making it difficult to make thin incisions. To overcome this, the XRD analysis method is used [28], [29]. This technique is useful for determining fine altered minerals that cannot be seen petrographically, such as clay or phyllosilicate minerals. XRD analysis aims to determine the type of minerals present in the alteration sample, with eight samples. XRD analysis was carried out entirely by the laboratory of Gadjah Mada University, Yogyakarta.

XRF (X-ray fluorescence) is a geochemical analysis used to determine the chemical composition of major elements in host rock and minerals [30]. It was conducted to determine the elements associated with gold and the major elements in gold deposits. PT Intertek Utama Services fully carried out the XRF analysis. XRD analysis was carried out on samples GB.04, GB.05, GB.06, GB.07, GB.08, GB.09, GB.10, and GBT.11. ICP-OES analysis determines the chemical composition of minor trace elements, especially metals associated with gold [27], [31], [32]. PT Intertek Utama Services fully carries out this analysis activity. AAS analysis determines the gold content in the analysed sample [33]. PT Intertek Utama Services fully carries out this AAS analysis. AAS analysis was performed to determine the gold content (Au), XRF analysis to determine major elements, and ICP-OES analysis to determine trace elements. The detection limit for XRF typically ranges from 10 ppm to 1% for heavy elements, with detectable analysis concentrations ranging from 0.01% to 100%, depending on the sample type and the sensitivity of the instrument. The detection limit for ICP OES can range from 0.1 ppb to 10 ppm for various elements, with detectable analysis concentrations ranging from 0.1 ppm to 1000 ppm, depending on the component being analysed. The analysis concentration for AAS typically ranges from 0.1 ppm to 1000 ppm, depending on the type of element being analysed.

## 3. Results And Discussion

### 3.1 Metamorphic Facies

Petrographic analysis determined the type of metamorphic facies present in the host rock of the gold deposit. Petrographic analysis is also useful for determining the texture, structure, and mineral composition of rocks. A mineral association found in rock samples was utilised to determine the type of facies. The mineral association was then plotted on a metamorphic facies diagram to determine the kind of facies and rock paragenesis. A total of three metamorphic rock samples were taken in the field. Based on the petrological analysis of the rocks, there was one sample of the phyllite-type rock and two samples of the muscovite schist-type rock.

#### *3.1.1 Phyllite*

Phyllite rock in the GB.01 rock sample microscopically has a transparent absorption colour, mineral size 0.06-0.6 mm, hypidiomorph-xenomorph mineral form, blackish grey interference colour, foliation structure, special blastophylitic texture. The structure type of this rock is foliated. The mineral composition comprises 35% quartz, 25% biotite, and 40% clay material. Quartz minerals exhibit a transparent colour with a hypidiomorph-xenomorph form, pleochroism (-), size 0.06-0.6 mm, low relief, weak intensity, white interference colour, wavy darkness. Biotite minerals are brownish with mineral size 0.1-0.6 mm, hypidiomorph-xenomorph form, dichotic pleochroic, brown interference colour, and parallel darkness type. The clay material is brownish with low relief, grain size <0.02 mm, and interference colour is brownish grey.

#### *3.1.2 Muscovite Schist*

Muscovite Schist is found in the GB.02 rock sample, which microscopically exhibits a transparent-blackish colour, mineral size 0.04-0.2 mm, idiomorphic-xenomorphic mineral form, yellow-bluish interference colour, porphyroblastic texture. The structure type of this rock

is foliated. The mineral composition comprises 25% muscovite, 40% chlorite, 25% quartz, and 10% opaque mineral. The muscovite mineral exhibits a transparent absorption colour with a sheet-like form, pleochroism (-), a mineral size of 0.04-0.2 mm, low relief, weak intensity, perfect cleavage in one direction, and an interference colour of yellowish orange, with an oblique type of darkness. The quartz mineral exhibits a transparent absorption colour with a hypidiomorphic-xenomorphic mineral form, pleochroism (-), mineral size 0.06–0.18 mm, low relief, weak intensity, cleavage (-), interference colour of blue-white, with a type of darkness that is wavy. Chlorite Mineral Shows transparent absorption colour with hypidiomorph-xenomorph mineral form, pleochroism (-), mineral size 0.08-0.1 mm, low relief, weak intensity, cleavage (-), light blue-reddish interference colour. At the same time, the type of darkness is oblique. Opaque Mineral shows black colour on Nicol parallel to the shape of opaque grains and mineral size 0.06-0.18 mm.

**Table 1:** The presence of quartz and calcite minerals is the green schist facies, according to Spear [34], [35]

| Facies | Metamorphic Rock Mineral Assemblage |
|---|---|
| Zeolite | Zeolites: Especially Laumunite, Wairakite, Analcime |
| Prehnite-Pumpellyite | Prehinite + Pumpellyite (Chlorite + Albite) |
| Green Schist | Chlorite + Albite + Epidote (or Zoisite) + Quartz + Actinolite |
| Amphibolite | Hornblende + Plagioclase (Oligoclase-andesine) + Garnet |
| Granulit | Orthopyroxene + Clinopyroxene + Plagioclase + Garnet + Hornblende |
| Blue Schist | Glaucophane + Lawsonite or epidote (Albite + Chlorite) |
| Eclogite | Pyralspite Garnet + Omphacitic Pyroxene (+ Kyanite) |
| Contact Facies | The mineral assemblages in the Contact Facies do not differ significantly. substantial of facies in higher pressure areas |

In the GB.03 rock sample, muscovite schist rock is also found, which microscopically shows a transparent to blackish colour, with mineral sizes ranging from 0.04 to 0.2 mm, a hypidiomorph-xenomorph mineral form, a yellow-bluish interference colour and porphyroblastic texture. The structure type of this rock is foliation-schistose. The mineral composition consists of 30% muscovite, 25% quartz, 35% chlorite and 10% opaque mineral. Quartz mineral shows transparent absorption colour, sheet mineral form, pleochroism (-), mineral size 0.06-0.1 mm, low relief, weak intensity, perfect cleavage in 1 direction, yellowish orange interference colour, oblique darkness type. Quartz mineral shows transparent absorption colour, hypidiomorph-xenomorph mineral form, pleochroism (-), mineral size 0.04-0.1 mm, low relief, weak intensity, cleavage (-), blue-white interference colour, wavy darkness type. Chlorite mineral shows transparent absorption colour, hypidiomorph-xenomorph mineral form, pleochroism (-), mineral size 0.08-0.2 mm, low relief, weak intensity, cleavage (-), light blue-reddish interference colour, oblique darkness type. Opaque myelin shows a black colour on parallel Nicol and crosses Nicol with grain shape, opacity, and a size of 0.04-0.12 mm. From

the results of petrographic analysis, a typical mineral set is used to determine the type of host-rock facies of gold deposits. The typical mineral types found at the research location consist of chlorite and quartz minerals. According to the table of mineral sets in metamorphic facies [34], [35], the type of facies found in the research area is the Greenschist facies.

Greenschist facies is formed in a regional metamorphic zone with a wide distribution and depth from 6 km to 33 km and a pressure between 2 and 11 kbar [34], [35]. The temperature ranges from 200 °C to 430 °C. Field observations reveal that the metamorphic rocks in the research area exhibit distinct characteristics, with the presence of quartz vein inserts in the rock foliation and quartz veins that cut the rock foliation. The presence of quartz veins that intersect and cut the foliation is visible in Figure 3.

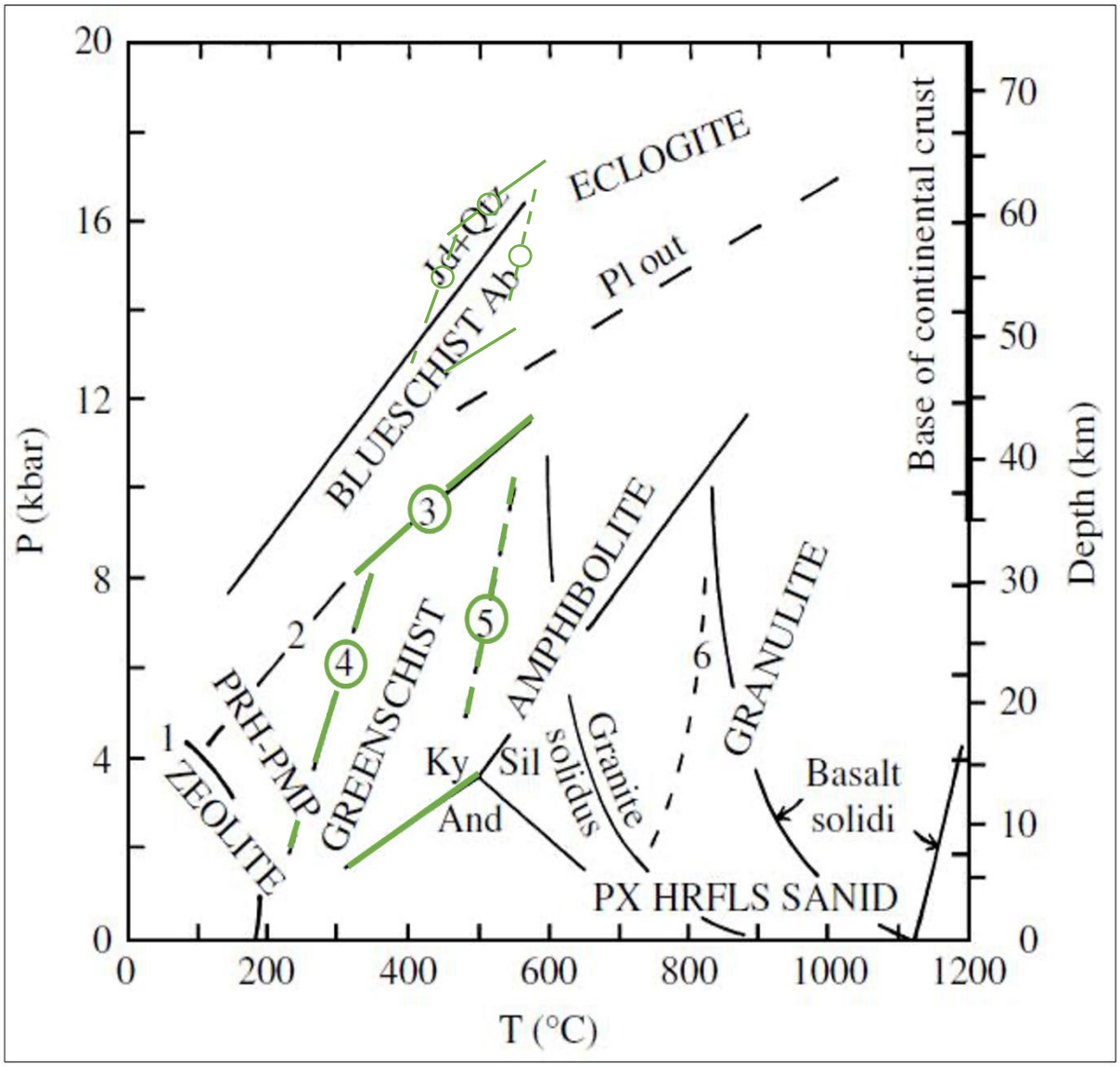


**Figure 2:** The green line shows the metamorphic facies of the research location, namely Green Schist (modification of the metamorphic facies according to Best [36]).

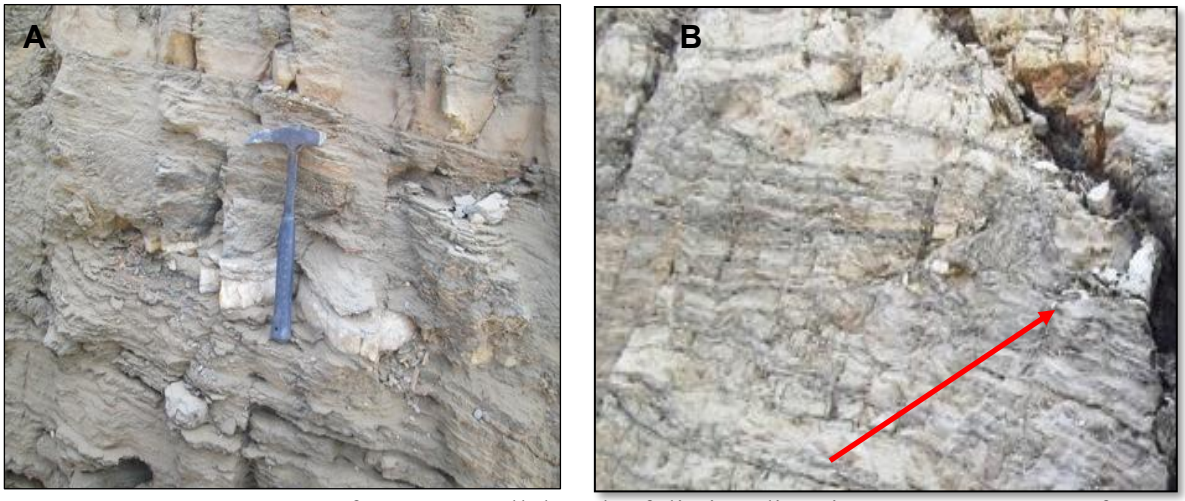


**Figure 3:** A. Occurrence of quartz parallel to the foliation direction. B. Occurrence of quartz intersecting the foliation direction

### 3.2 Alteration Type

The alteration type was identified based on the XRD and petrographic analysis results. In contrast, petrographic analysis was carried out on sample GB.07. The difference in the kind of analysis is due to the soft sample material, which cannot be thinly sectioned for petrographic analysis; therefore, XRD analysis was performed. Based on XRD and petrographic analysis, the alteration zones developed in the research area are classified into four alteration types. Four alteration types are found: silicic type, sericitization type, argillic type, and chloritization type. The above alteration types will be described based on the characteristic minerals found.

#### *3.2.1 Silicic Type*

The Silicic type is found in samples GB.04, GB.05, GB.06, and GB.07, characterised by dominant quartz minerals (Figure 4). The quartz mineral sample shows a reddish-brown colour, indicating that the quartz mineral contains metal due to oxidation (Figure 4). Silica is formed at a temperature of 100-200°C [37]. Community mining activities are carried out in the Silicic zone.

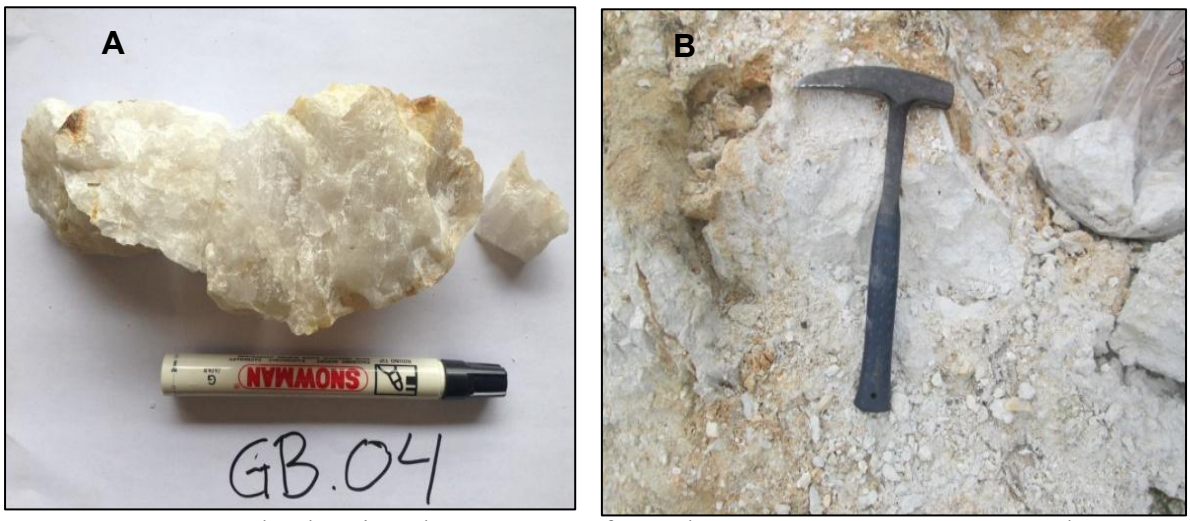


**Figure 4:** A. Example showing the presence of metal content. B. Outcrop Example GB.05, silicic alteration is characterised by dominant quartz minerals.

3.2.2 Sericitization Type

The results of XRD analysis show that Sericite type is found in samples GB.08, GB.09, GB.10, and GB.11. The presence of muscovite minerals characterises this alteration. Formed at temperatures >250°C. Crystallisation in illite and sericite increases with increasing temperature [37]. Sample images are shown in Figure 5.

3.2.3 Argillic Type

In the GB.07 sample with petrographic analysis, clay minerals characterise the presence of Argillic alteration. Clay minerals show a brownish-black colour with low relief, grain size <0.3 mm, and interference colour is brownish grey. Thin sections also show the presence of quartz veinlets and opaque minerals (Figure 6). Clay minerals are formed in areas with shallow depths, with temperatures <200-250°C [37].

3.2.4 Chloritization Type

The chloritization type is characterised by the presence of chlorite minerals associated with quartz [38]. Based on the results of XRD analysis, this mineral is found in samples GB.08, GB.09, GB.10, and GB.11. Chlorite is formed at a temperature of 200-250°C [37].

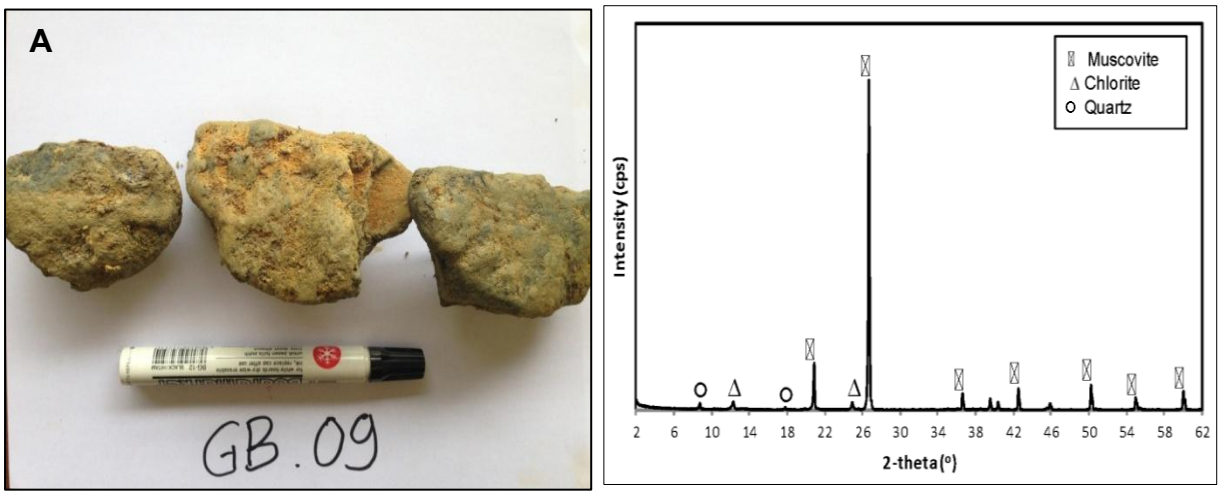


**Figure 5:** A. Example GB.09, Sericitization alteration. B. XRD analysis shows the presence of muscovite.

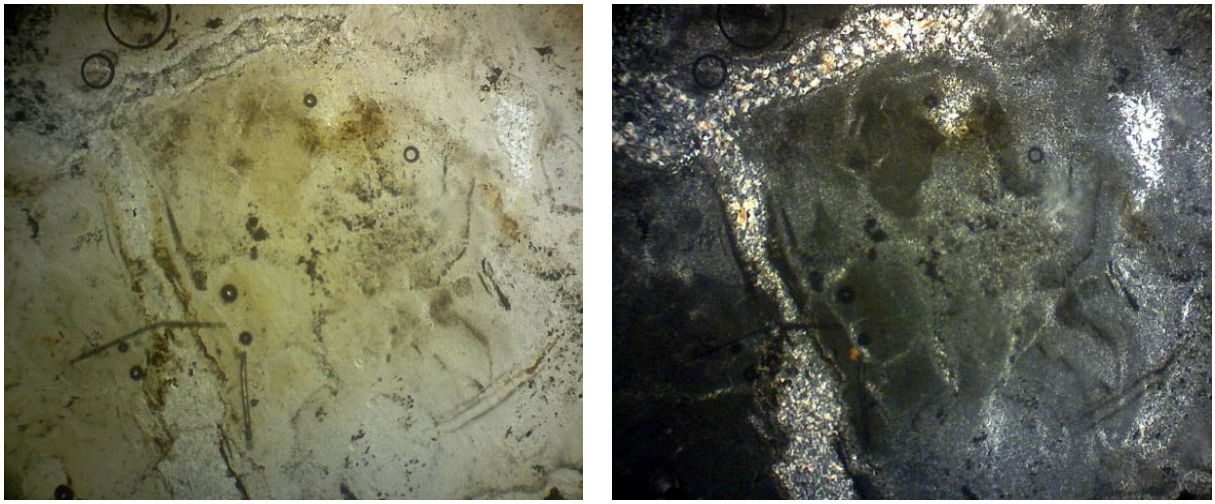

**Figure 6:** A. Parallel Nikol shows quartz veinlet found in 2 B. B. Clay minerals found in 2F, Opaque minerals found in 3E

### 3.3 Mineralisation

The mineralogical process of the research area is generally formed in quartz veins, with oxidation in quartz minerals marked by a blackish-brown colour. There are also white to clear quartz minerals, which are usually barren. These minerals are found in abundance in the research area. Observation activities in a 30-meter-deep community mine (shaft) (GB.11) showed quartz veins with a crustiform banding texture. The quartz veins in the shaft are between 40 and 50 cm thick. The quartz veins also show alternating quartz bands and sulfide bands. In other shafts, small quartz veins intersect and form stockwork. The high level of weathering causes the material to become soft. Based on the results of the AAS analysis, samples taken from the shaft (GB.12) have a high gold content, 5.9 g/t. This mineralisation zone is surrounded by argillic, chloritization, silicic, and sericitization alteration (Figure 7 B).

### 3.4 Gold Content and Geochemistry

To determine the gold content and geochemistry, which were then associated with the type of gold deposits in the research area. The number of samples analysed in the Gunung Botak area was seven samples, namely GB.04, GB.06, GB.08, GB.09, GB.10, GB.11, and GB.12. For more details, see Table 2. Based on the results of geochemical analysis (XRF), the $SiO_2$ content shows a very high percentage, ranging from 74.15% to 97.43%. This indicates the presence of gold associated with gangue minerals, namely Quartz. MgO content is also found in samples GB.08, GB.09, GB.10, and GB.11 (Figure 8). The graph shows that the $SiO_2$ graph is inversely proportional to the MgO content. If the $SiO_2$ content increases, the MgO content decreases, and vice versa. If the MgO content increases, the $SiO_2$ content decreases. The $SiO_2$ and MgO graphs in Figure 8 show a nonlinear graph.

The gold content varies in each sample analysis, ranging from 0.23 g/ton to 5.9 g/ton. Significant gold content is seen in sample GB.09, which has an Au content of 1.83 g/ton. The high gold content is found in sericitic, argillic, and propylitic alteration types. The data in Table 2 indicates that the Ag element is associated with Au, although it shows a relatively low content of <0.1 g/ton – 0.2 g/ton (Figure 8). Based on the logarithmic graph of the linear function in Figure 8, the graph of the Au and Ag elements shows that the Ag element content does not accompany the increase in the Au element content and shows a non-linear graph. The Ag content shows a flat graph and remains unaffected by changes in the Au element content. Likewise, the Mn element shows a nonlinear graph.

The elements Cr and Cu show significant levels. This can be seen in the Cr content of 7g/ton – 18 g/ton and the Cu content of 2g/ton–35 g/ton. The presence of the Cu element results from increased pressure and temperature, a diagenetic change in the metamorphic facies known as the precursor principal name [39]. The Cu and Au elements exhibit similar behaviour in graphs and are linear. When Au enrichment occurs, the Cu content also experiences enrichment, and the graph will show a linear trend (Figure 8). Quartz veins show enrichment in the elements As, Ba, K, Sb, and Te, which vary; Pb concentrations are generally slightly higher than those in regional conditions.

Data showing the enrichment of Au, As, and Sb, along with a linear graph, are characteristics of orogenic deposits [40], [41]. As and Sb can be used as pathfinders to find Au [42]. The enrichment of As, Sb, and Hg also indicates orogenic deposit mineralisation [11]. The enrichment graph shows it occurring in the elements As and Sb. Based on geochemical analysis data, the research area has geochemical characteristics, namely polymetallic mineralisation.

The correlation between gold and elements like As, Cu, alumina, and magnesia is largely a result of hydrothermal processes that cause both gold and these elements to precipitate from mineralising fluids under similar conditions. Arsenic and copper, in particular, are directly involved in the formation of gold-bearing minerals, while alumina and magnesia often serve as indicators of the geological environment that facilitates gold mineralisation [36], [43]

**Figure 7:** A. Quartz Vein with a 40-50 cm thickness and crustiform banding texture (alternation of quartz and sulfide). B The mineralised zone in the shaft shows vein stockwork that indicates an alteration in grey, greenish, yellow, and white colours (indications of chlorite, quartz, and silicic)

**Table 2:** Results of geochemical analysis (XRF analysis, ICP-OES analysis and AAS analysis)

| No. Sampel<br>Tipe sampel | GB.04<br>Float qz | GB.06<br>Vein qz | GB.08<br>Vein | GB.09<br>Vein | GB.10<br>Vein | GB.11<br>Vein | GB.12<br>Ore vein | DL |
|---|---|---|---|---|---|---|---|---|
| Major oxides (wt.%) | | | | | | | | |
| $SiO_2$ | 97.43 | 96.71 | 82.84 | 79.66 | 82.72 | 74.15 | NA | 0.01 |
| $TiO_2$ | <0.01 | 0.02 | 0.49 | 0.47 | 0.42 | 0.75 | NA | 0.01 |
| $Al_2O_3$ | 0.04 | 0.24 | 10.49 | 11.62 | 9.49 | 15.72 | NA | 0.01 |
| $Fe_2O_3$ | 2.61 | 2.65 | 1.43 | 2.37 | 1.87 | 1.74 | NA | 0.01 |
| MnO | 0.026 | 0.021 | 0.010 | 0.005 | 0.006 | 0.005 | NA | 0.005 |
| MgO | <0.01 | <0.01 | 0.15 | 0.22 | 0.27 | 0.27 | NA | 0.01 |
| CaO | 0.02 | <0.01 | 0.01 | <0.01 | 0.02 | 0.01 | NA | 0.01 |
| $Na_2O$ | <0.01 | <0.01 | 0.06 | 0.1 | 0.08 | 0.16 | NA | 0.01 |
| $K_2O$ | 0.01 | 0.03 | 0.94 | 1.52 | 1.64 | 2.32 | NA | 0.01 |
| $P_2O_5$ | 0.01 | 0.01 | 0.014 | 0.012 | 0.015 | 0.018 | NA | 0.001 |
| $Cr_2O_3$ | <0.05 | <0.05 | 0.036 | 0.044 | 0.028 | 0.011 | NA | 0.005 |
| LOI | -0.7 | -0.6 | 3,4 | 3,4 | 2.8 | 4.2 | NA | 0.1 |
| S | <0.002 | <0.002 | 0.006 | <0.002 | <0.002 | 0.003 | NA | 0.002 |
| Trace elements (ppm) | | | | | | | | |
| Au | <0.01 | 0.31 | 0.23 | 1.83 | 0.85 | 0.76 | 5.9 | 0.01 |
| Ag | <0.1 | 0.2 | <0.1 | 0.1 | <0.1 | <0.1 | NA | 0.1 |
| Al | 0.02 | 0.04 | 1.19 | 1.25 | 0.56 | 1.02 | NA | 0.01 |
| As | <2 | 51 | 92 | 228 | 191 | 153 | NA | 2 |
| Ba | 1 | 2 | 21 | 36 | 29 | 38 | NA | 1 |
| Bi | <2 | <2 | <2 | <2 | <2 | <2 | NA | 2 |
| Ca | 0.01 | <0.01 | <0.01 | <0.01 | <0.01 | <0.01 | NA | 0.01 |
| Cd | <0.2 | <0.2 | <0.2 | <0.2 | <0.2 | <0.2 | NA | 0.2 |
| Co | 2 | 2 | 1 | 2 | 1 | 1 | NA | 1 |
| Cr | 18 | 16 | 15 | 15 | 7 | 11 | NA | 1 |
| Cu | 2 | 2 | 13 | 35 | 16 | 18 | NA | 1 |
| Fe | 1.79 | 1.87 | 0.83 | 1.66 | 1.3 | 1.02 | NA | 0.01 |
| Ga | 2 | 2 | 3 | 4 | 3 | 4 | NA | 2 |
| K | <0.01 | 0.01 | 0.1 | 0.2 | 0.15 | 0.22 | NA | 0.01 |
| La | <1 | <1 | 4 | 4 | 10 | 21 | NA | 1 |
| Li | <1 | <1 | 1 | 2 | 1 | 1 | NA | 1 |
| Mg | 0.01 | <0.01 | 0.01 | 0.02 | 0.01 | 0.02 | NA | 0.01 |
| Mn | 182 | 159 | 16 | 22 | 8 | 10 | NA | 1 |
| Mo | 1 | <1 | <1 | 1 | <1 | 1 | NA | 1 |
| Na | 0.01 | <0.01 | 0.01 | 0.01 | 0.01 | 0.01 | NA | 0.01 |
| Nb | <1 | <1 | <1 | <1 | <1 | <1 | NA | 1 |
| Ni | 4 | 3 | 1 | 1 | <1 | <1 | NA | 1 |
| Pb | <2 | <2 | 2 | 3 | 4 | 6 | NA | 2 |
| Sb | 1 | 9 | 20 | 26 | 33 | 26 | NA | 1 |
| Sc | <1 | <1 | 3 | 3 | 2 | 5 | NA | 1 |
| Se | <10 | <10 | <10 | <10 | <10 | <10 | NA | 10 |
| Sn | <5 | <5 | <5 | <5 | <5 | <5 | NA | 5 |
| Sr | 1 | <1 | 3 | 4 | 3 | 7 | NA | 1 |
| Ta | <5 | <5 | <5 | <5 | <5 | <5 | NA | 5 |
| Te | <5 | <5 | <5 | <5 | <5 | <5 | NA | 5 |
| Ti | <0.01 | <0.01 | 0.01 | <0.01 | <0.01 | <0.01 | NA | 0.01 |

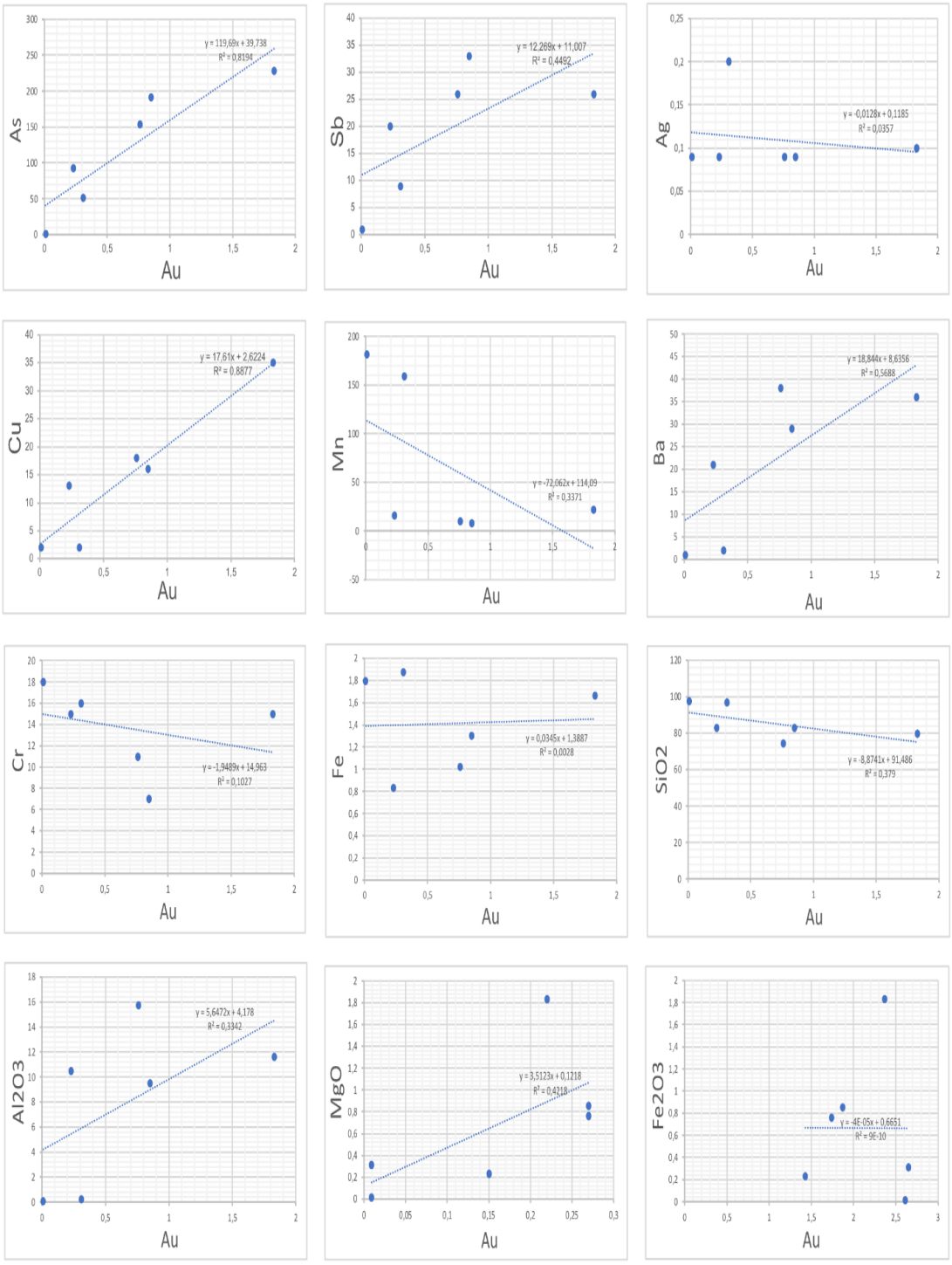


**Figure 8:** Linear function logarithmic graph (Au to As, Sb, Ag, Cu, Mn, Ba, Cr, Fe, $SiO_2$, $Al_2O_3$, MgO, $Fe_2O_3$)

### 3.5 Gold Deposit Types

The type of deposit found in the research area. Based on the results of the discussion above, it can be concluded that the type of deposit is an orogenic gold deposit. This can be seen from the kind of host-rock facies of the gold deposit. The type of facies is greenschist facies [44], [45], [46]. Stüwe [41] state that regional metamorphism processes usually affect orogenic gold deposits, forming greenschist facies metamorphic rocks. Metamorphic rocks, as host rocks, are

formed at depths between 6 km and 33 km with pressures between 6 kbar and 11 kbar and temperatures between 200°C and 430°C. The types of alteration in chloritization and sericitization are types of alteration commonly found in orogenic gold deposits [38]. Ore mineralisation hosted by quartz gangue minerals in the form of veins indicates orogenic (mesothermal) type deposits. The geochemical characteristics of quartz veins show enrichment in As, Ba, Sb, and Te, with varying Pb concentrations. All these characteristics characterise orogenic-type gold deposits [40], [41], [47], [48]. The presence of the elements Au, As, Pb, and Sb is also related to orogens [49], [50], [51], [52], [53]. Orogenic gold deposits are always associated with the presence of anomalous Pb element content [54], [55].

The gold deposition environment of the research area is interpreted based on facies analysis data (greenschist facies) associated with geochemical data. The gold deposit model used is the orogenic type of gold deposit model, according to Goldfarb [48] the geochemical analysis results show significant Au, Sb, As and Te in the model. The location in the mesozonal zone is indicated by the presence of significant Au, Sb, and As, as well as Te, which are then plotted. [48]. The zone is formed at a depth of 5Km-10Km [56]. The temperature of gold formation based on the alteration temperature ranges from 100°C to 250°C. According to Goldfarb (Figure 9), the model is a modified model based on the orogenic gold deposit model [48].

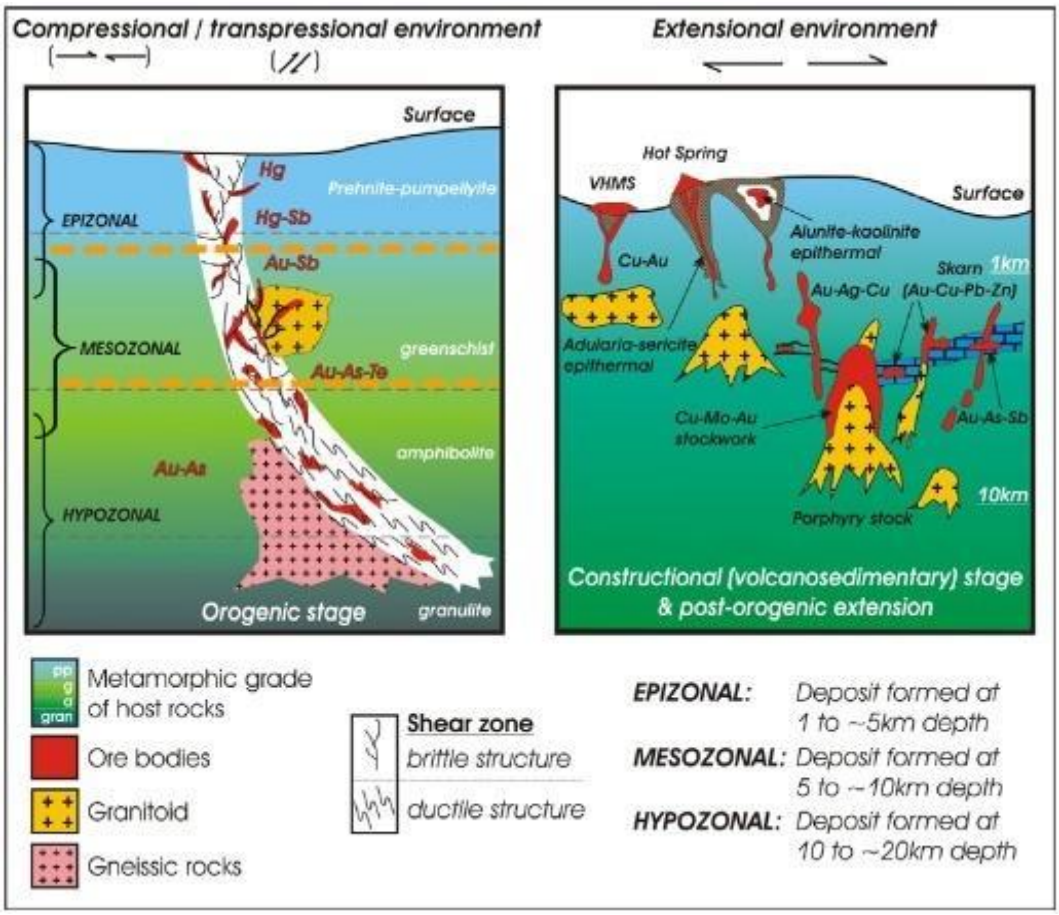


**Figure 9:** The orange dashed line on the left shows the range of environmental formation of orogenic-type gold mineralisation in the research area, based on the results of the genetic model plot of orogenic-type gold deposits [48], formed in the Mesozonal zone with a depth of between 5-10 km.

## 4 Conclusion

The following conclusions can be drawn: Host-rock gold deposits on Buru Island are metamorphic rocks, especially in the Mount Botak area. These metamorphic rocks include phyllite and muscovite schist, formed in the greenschist facies process. These facies are formed at depths from 6 km to 33 km and at pressures between 2 kbar and 11 kbar. The temperature ranges from 200 °C to 430 °C. The types of alteration found in the research area, which are associated with and bordering the mineralisation zones, are silicic, sericitization, argillic, and chloritization. The mineralisation characteristics are generally in the form of quartz veins with oxidation processes (supergene). The texture of mineralisation is characterised by crustiform banding (alternating quartz and sulfide) and a little vein stockwork. Geochemical analysis data indicate that the research area has geochemical characteristics, namely polymetallic mineralisation. The gold (Au) content ranges from 0.23 to 5.9 g/ton. Enrichment in gold content was not accompanied by silver (Ag) content enrichment. Element enrichment is found in As 228 ppm and Sb 33 ppm. Based on the results and discussions on host rock, alteration type, mineralisation type, geochemical characteristics of elements, and ore content, it is concluded that the type of deposit in the research area is an orogenic gold deposit. Formed in the Mesozonal environment at a depth of 5-10 Km with a temperature between 100°C-250°C. The implications for Orogenic gold exploration activities in this study area include several important aspects. Exploration must focus on depths of 5-10 km, utilising drilling and geophysical mapping to identify potential mineralisation zones.

**References**


[1] A. Basuki, D. Aditya Sumanagara, and D. Sinambela, "The Gunung Pongkor gold-silver deposit, West Java, Indonesia," *J Geochem Explor*, vol. 50, no. 1–3, pp. 371–391, Mar. 1994, doi: 10.1016/0375-6742(94)90032-9.

[2] S. Prihatmoko and A. Idrus, "Low-sulfidation epithermal gold deposits in Java, Indonesia: Characteristics and linkage to the volcano-tectonic setting," *Ore Geol Rev*, vol. 121, p. 103490, Jun. 2020, doi: 10.1016/J.OREGEOREV.2020.103490.

[3] A. D. Titisari, D. Phillips, I. W. Warmada, Hartono, and A. Idrus, "40Ar/39Ar geochronology of the Pongkor low sulfidation epithermal gold mineralisation, West Java, Indonesia," *Ore Geol Rev*, vol. 119, p. 103341, Apr. 2020, doi: 10.1016/J.OREGEOREV.2020.103341.

[4] J. C. Carlile, G. R. Davey, I. Kadir, R. P. Langmead, and W. J. Rafferty, "Discovery and exploration of the Gosowong epithermal gold deposit, Halmahera, Indonesia," *J Geochem Explor*, vol. 60, no. 3, pp. 207–227, Mar. 1998, doi: 10.1016/S0375-6742(97)00048-4.

[5] T. P. Mernagh, C. Leys, and R. W. Henley, "Fluid inclusion systematics in porphyry copper deposits: The super-giant Grasberg deposit, Indonesia, as a case study," *Ore Geol Rev*, vol. 123, p. 103570, Aug. 2020, doi: 10.1016/J.OREGEOREV.2020.103570.

[6] T. P. Mernagh and J. Mavrogenes, "Significance of high temperature fluids and melts in the Grasberg porphyry copper-gold deposit," *Chem Geol*, vol. 508, pp. 210–224, Mar. 2019, doi: 10.1016/J.CHEMGEO.2018.09.040.

[7] R. W. Henley *et al.*, "Potassium silicate alteration in porphyry copper-gold deposits: a case study at the giant maar-diatreme hosted Grasberg deposit, Indonesia," *Journal of Volcanology and Geothermal Research*, vol. 432, p. 107710, Dec. 2022, doi: 10.1016/J.JVOLGEORES.2022.107710.

[8] A. Idrus, J. Kolb, and F. M. Meyer, "Chemical Composition of Rock-Forming Minerals in Copper–Gold-Bearing Tonalite Porphyries at the Batu Hijau Deposit, Sumbawa Island, Indonesia: Implications for Crystallisation Conditions and Fluorine–Chlorine Figacity," *Resource Geology*, vol. 57, no. 2, pp. 102–113, Jun. 2007, doi: 10.1111/J.1751-3928.2007.00010.X.

[9] A. Idrus, J. Kolb, and F. M. Meyer, "Mineralogy, Lithogeochemistry and Elemental Mass Balance of the Hydrothermal Alteration Associated with the Gold-rich Batu Hijau Porphyry Copper Deposit, Sumbawa Island, Indonesia," *Resource Geology*, vol. 59, no. 3, pp. 215–230, Sep. 2009, doi: 10.1111/J.1751-3928.2009.00092.X.

[10] H. Hasria, A. Idrus, and I. W. Warmada, "The Metamorphic Rocks-Hosted Gold Mineralisation At Rumbia Mountains Prospect Area In The Southeastern Arm of Sulawesi Island, Indonesia," *Journal of Geoscience, Engineering, Environment, and Technology*, vol. 2, no. 3, pp. 217–223, Sep. 2017, doi: 10.24273/JGEET.2017.2.3.434.

[11] A. Idrus *et al.*, "Some Key Features and Possible Origin of the Metamorphic Rock-Hosted Gold Mineralisation in Buru Island, Indonesia," *Indonesian Journal on Geoscience*, vol. 1, no. 1, pp. 9–19, Apr. 2014, doi: 10.17014/IJOG.1.1.9-19.

[12] A. Idrus *et al.*, "Metamorphic rock-hosted orogenic gold deposit style at Bombana (Southeast Sulawesi) and Buru Island (Maluku): Their key features and significances for gold exploration in Eastern Indonesia," *Journal of Geoscience, Engineering, Environment, and Technology*, vol. 2, no. 2, pp. 124–132, Jun. 2017, doi: 10.24273/JGEET.2017.2.2.291.

[13] A. Permatasari, "Elemental Mass Balance Calculation of the Hydrothermal Alteration in Awak Mas Gold Deposit, Sulawesi Island, Indonesia," *IOP Conf Ser Earth Environ Sci*, vol. 1437, no. 1, 2024, doi: 10.1088/1755-1315/1437/1/012007.

[14] A. Y. A. Hakim, "Formation of epizonal gold mineralisation within the Latimojong Metamorphic Complex, Sulawesi, Indonesia: Evidence from mineralogy, fluid inclusions and Raman spectroscopy," *Ore Geol Rev*, vol. 97, pp. 88–108, 2018, doi: 10.1016/j.oregeorev.2018.05.001.

[15] E. Ernowo, "Elemental Gains and Losses during Hydrothermal Alteration in Awak Mas Gold Deposit, Sulawesi Island, Indonesia: Constraints from Balanced Mineral Reactions," *Minerals*, vol. 12, no. 12, 2022, doi: 10.3390/min12121630.

[16] E. Ernowo, "Hydrothermal alteration and gold mineralisation of the Awak Mas metasedimentary rock-hosted gold deposit, Sulawesi, Indonesia," *Ore Geol Rev*, vol. 113, 2019, doi: 10.1016/j.oregeorev.2019.103083.

[17] M. Z. Tuakia, "Geological and Geochemical Characteristics of Gold Mineralisation in the Salu Bulo Prospect, Sulawesi, Indonesia," *Resource Geology*, vol. 69, no. 2, pp. 176–192, 2019, doi: 10.1111/rge.12193.

[18] A. Idrus, S. Mansur, A. Ahmad, R. Rahmayuddin, and A. Abdul, "Occurrences and Characteristics of Gold Mineralisation in Rampi Block Prospect, North Luwu Regency, South Sulawesi Province, Indonesia," *Journal of Applied Geology*, vol. 1, no. 2, pp. 63–70, Jul. 2016, doi: 10.22146/JAG.26962.

[19] A. Idrus, I. Nur, I. W. Warmada, and F. Fadlin, "Metamorphic Rock-Hosted Orogenic Gold Deposit Type as a Source of Langkowala Placer Gold, Bombana, Southeast Sulawesi," *Indonesian Journal on Geoscience*, vol. 6, no. 1, pp. 43–49, Mar. 2011, doi: 10.17014/IJOG.6.1.43-49.

[20] H. Hasria, "Orogenic Gold Deposit in Metamorphic Rocks: Minerals and Structural Control at Rarowatu Area, Southeastern Arm of Sulawesi, Indonesia," *Iraqi Geological Journal*, vol. 56, no. 1, pp. 16–31, 2023, doi: 10.46717/igj.56.1B.2ms-2023-2-10.

[21] S. Tjokrosapoetra, T. Budhitrisna, and E. Rusmana, "Geological Map of Buru Quadrangle, Maluku, Scale 1: 250,000," Bandung, 1993.

[22] K. Linthout, H. Helmers, J. Sopaheluwakan, and E. S. Nila, "Metamorphic complexes in Buru and Seram, Northern Banda Arc," *Netherlands Journal of Sea Research*, vol. 24, no. 2–3, pp. 345–356, Nov. 1989, doi: 10.1016/0077-7579(89)90160-9.

[23] Y. Wang, "Orogenic Gold Metallogenic System in North Margin of Yangtze Block: Preliminary Study on Tectonic Evolution and Mineralisation," *IOP Conf Ser Earth Environ Sci*, vol. 300, no. 2, 2019, doi: 10.1088/1755-1315/300/2/022144.

[24] A. Almasi, "Evaluation of structural and geological factors in orogenic gold type mineralisation in the Kervian area, North-West Iran, using airborne geophysical data," *Exploration Geophysics*, vol. 45, no. 4, pp. 261–270, 2014, doi: 10.1071/EG13053.

[25] A. B. Pour, "Structural Mapping of the Bentong-Raub Suture Zone Using PALSAR Remote Sensing Data, Peninsular Malaysia: Implications for Sediment-hosted/Orogenic Gold Mineral Systems Exploration," *Resource Geology*, vol. 66, no. 4, pp. 368–385, 2016, doi: 10.1111/rge.12105.

[26] S. O. Sanusi, "Mapping of Orogenic Gold Mineralisation Potential in the Kushaka Schist Belt, Northcentral Nigeria: Insights from Point Pattern, Kernel Density, Staged-Factor, and Fuzzy

AHP Modeling Techniques," *Earth Systems and Environment*, 2024, doi: 10.1007/s41748-024-00427-8.

[27] M. I. A. Halim, M. F. Safian, E. Elias, and S. S. Shazali, "Identification of gunshot residue from trace element by using ICP/OES identifikasi residu tembakan pistol daripada unsur surih menggunakan ICP/OES," *2013 IEEE Symposium on Computers & Informatics (ISCI)*, 2013, doi: 10.1109/isci.2013.6612409.

[28] A. B. Thamsi, M. Aswadi, H. Anwar, H. Bakri, M. Hardin Wakila, and A. F. Heriansyah, "Karakteristik Mineraloid Opal Limbong, Kabupaten Luwu Utara, Provinsi Sulawesi Selatan," *Jurnal Geomine*, vol. 8, no. 3, p. 220, Feb. 2021, doi: 10.33536/JG.V8I3.735.

[29] A. B. Thamsi, A. A. Budiman, E. P. Umar, and H. Harwan, "Host-rock characteristics and geochemistry of the Rongkong Opal-C Mineraloid, North Luwu Regency, South Sulawesi Province, Indonesia," *Gospodarka Surowcami Mineralnymi – Mineral Resources Management*, vol. 40, no. 1, pp. 233–246, Mar. 2024, doi: 10.24425/GSM.2024.149301.

[30] M. H. Wakila, S. Nompo, N. Jafar, A. B. Thamsi, A. S. Munir, and A. F. Heriansyah, "Analysis of Cobalt Distribution and Co-Ni Correlation in Nickel Laterite Zonation in Tropical Region," *The Iraqi Geological Journal*, vol. 57, no. 2, pp. 205–218, Aug. 2024, doi: 10.46717/IGJ.57.2B.14MS-2024-8-24.

[31] J. Zhang *et al.*, "LA-ICP-MS trace element analysis of pyrite from the Chang'an gold deposit, Sanjiang region, China: Implication for ore-forming process," *Gondwana Research*, vol. 26, no. 2, pp. 557–575, Sep. 2014, doi: 10.1016/J.GR.2013.11.003.

[32] A. B. Thamsi, M. H. Wakila, L. Ahmad, and M. Aswadi, "Geochemistry of Iron Ore in Kadong-Kadong, South Sulawesi, Indonesia," *The Iraqi Geological Journal*, vol. 58, no. 1, pp. 1–17, Apr. 2025, doi: 10.46717/IGJ.2025.58.1D.1.

[33] A. Tonggiroh and I. Nur, "Geochemical correlation of gold placer and indication of Au-Cu-Pb-Zn-Ag mineralisation at Parigi Moutong, Central Sulawesi, Indonesia," *J Phys Conf Ser*, vol. 1341, no. 5, p. 052003, Oct. 2019, doi: 10.1088/1742-6596/1341/5/052003.

[34] F. S. Spear, *Metamorphic phase equilibria and pressure-temperature-time paths*. America: Mineralogical Society of America, 1993.

[35] J. D. Winter, *An Introduction to Igneous and Metamorphic Petrology*. Prentice Hall, 2001. Accessed: Jan. 24, 2023. [Online]. Available: https://books.google.com/books/about/An_Introduction_to_Igneous_and_Metamorph.html?hl=id&id=5gJyQgAACAAJ

[36] S. X. Yang and N. Blum, "Arsenic as an indicator element for gold exploration in the region of the Xiangxi Au–Sb–W deposit, NW Hunan, PR China," *J Geochem Explor*, vol. 66, no. 3, pp. 441–456, Sep. 1999, doi: 10.1016/S0375-6742(99)00044-8.

[37] G. J. Corbett and T. M. Leach, "Southwest Pacific Rim Gold-Copper Systems: Structure, Alteration, and Mineralisation," *Southwest Pacific Rim Gold-Copper Systems*, Feb. 1998, doi: 10.5382/SP.06.

[38] A. M. Evans, *Ore Geology and Industrial Minerals An Introduction*. Oxford: Wiley, 2013. Accessed: Jan. 24, 2023. [Online]. Available: https://www.wiley.com/en-us/Ore+Geology+and+Industrial+Minerals%3A+An+Introduction%2C+3rd+Edition-p-9781118685020

[39] F. Pirajno, *Hydrothermal Mineral Deposits*. Germany: Springer Berlin Heidelberg, 1992. doi: 10.1007/978-3-642-75671-9.

[40] D. I. Groves, R. J. Goldfarb, M. Gebre-Mariam, S. G. Hagemann, and F. Robert, "Orogenic gold deposits: A proposed classification in the context of their crustal distribution and relationship to other gold deposit types," *Ore Geol Rev*, vol. 13, no. 1–5, pp. 7–27, Apr. 1998, doi: 10.1016/S0169-1368(97)00012-7.

[41] D. I. Groves, R. J. Goldfarb, F. Robert, and C. J. R. Hart, "Gold Deposits in Metamorphic Belts: Overview of Current Understanding, Outstanding Problems, Future Research, and Exploration Significance," *Economic Geology*, vol. 98, no. 1, pp. 1–29, Jan. 2003, doi: 10.2113/GSECONGEO.98.1.1.

[42] H. Hasria, A. Idrus, and I. W. Warmada, "Alteration Alteration, Mineralisation and Geochemistry of Metamorphic Rocks Hosted Hydrothermal Gold Deposit at Rumbia Mountains, Bombana Regency, Southeast Sulawesi, Indonesia," *Journal of Geoscience,*

*Engineering, Environment, and Technology*, vol. 4, no. 2, p. 83, Jun. 2019, doi: 10.25299/jgeet.2019.4.2.2346.

[43] R. G. Skirrow, "Iron oxide copper-gold (IOCG) deposits – A review (part 1): Settings, mineralogy, ore geochemistry and classification," *Ore Geol Rev*, vol. 140, p. 104569, Jan. 2022, doi: 10.1016/J.OREGEOREV.2021.104569.

[44] Q. Wang, "Towards a universal model for orogenic gold systems: A perspective based on Chinese examples with geodynamic, temporal, and deposit-scale structural and geochemical diversity," *Earth Sci Rev*, vol. 224, 2022, doi: 10.1016/j.earscirev.2021.103861.

[45] D. Gaboury, "Parameters for the formation of orogenic gold deposits," *Applied Earth Science: Transactions of the Institute of Mining and Metallurgy*, vol. 128, no. 3, pp. 124–133, 2019, doi: 10.1080/25726838.2019.1583310.

[46] D. Xu, "Gold mineralisation in the Jiangnan Orogenic Belt of South China: Geological, geochemical and geochronological characteristics, ore deposit-type and geodynamic setting," *Ore Geol Rev*, vol. 88, pp. 565–618, 2017, doi: 10.1016/j.oregeorev.2017.02.004.

[47] D. I. Groves, M. Santosh, J. Deng, Q. Wang, L. Yang, and L. Zhang, "A holistic model for the origin of orogenic gold deposits and its implications for exploration," *Miner Depos*, vol. 55, no. 2, pp. 275–292, Feb. 2020, doi: 10.1007/S00126-019-00877-5/METRICS.

[48] R. J. Goldfarb, D. I. Groves, and S. Gardoll, "Orogenic gold and geologic time: a global synthesis," *Ore Geol Rev*, vol. 18, no. 1–2, pp. 1–75, Apr. 2001, doi: 10.1016/S0169-1368(01)00016-6.

[49] H. Li, D. P. Zhu, L. W. Shen, T. J. Algeo, and S. M. Elatikpo, "A general ore formation model for metasediment-hosted Sb-(Au-W) mineralisation of the Woxi and Banxi deposits in South China," *Chem Geol*, vol. 607, p. 121020, Sep. 2022, doi: 10.1016/J.CHEMGEO.2022.121020.

[50] S. M. Elatikpo, H. Li, B. Liu, and W. D. Zhang, "Metallogenesis of the Bakoshi-Kundila gold deposit in northern West Nigerian Subshield: Insights from pyrite chemical and sulfur isotopic compositions and zircon U-Pb geochronology," *Precambrian Res*, vol. 383, p. 106890, Dec. 2022, doi: 10.1016/J.PRECAMRES.2022.106890.

[51] K. F. Qiu, "The giant Zaozigou Au-Sb deposit in West Qinling, China: magmatic- or metamorphic-hydrothermal origin?," *Miner Depos*, vol. 55, no. 2, pp. 345–362, 2020, doi: 10.1007/s00126-019-00937-w.

[52] D. Wyman, "Orogenic gold and the mineral systems approach: Resolving fact, fiction and fantasy," *Ore Geol Rev*, vol. 78, pp. 322–335, 2016, doi: 10.1016/j.oregeorev.2016.04.006.

[53] R. J. Goldfarb, "Orogenic gold: Common or evolving fluid and metal sources through time," *Lithos*, vol. 233, pp. 2–26, 2015, doi: 10.1016/j.lithos.2015.07.011.

[54] Y. Chen, H. Li, C. Zheng, S. M. Elatikpo, S. Cheng, and W. Jiang, "Ore-forming process of the Haigou gold deposit in the eastern Central Asian Orogenic Belt, NE China: Constrains from EPMA and LA-ICP-MS analysis of Au-bearing pyrite," *Resource Geology*, vol. 72, no. 1, p. e12304, Jan. 2022, doi: 10.1111/RGE.12304.

[55] H. Li *et al.*, "Pyrite trace element and S-Pb isotopic evidence for contrasting sources of metals and ligands during superimposed hydrothermal events in the Dongping gold deposit, North China," *Miner Depos*, vol. 58, no. 2, pp. 337–358, Feb. 2023, doi: 10.1007/S00126-022-01128-W/METRICS.

[56] M. Gebre-Mariam, D. I. Groves, N. J. McNaughton, E. J. Mikucki, and J. R. Vearncombe, "Archaean Au-Ag mineralisation at Racetrack, near Kalgoorlie, Western Australia: a high crustal-level expression of the Archaean composite lode-gold system," *Miner Depos*, vol. 28, no. 6, pp. 375–387, Dec. 1993, doi: 10.1007/BF02431597/METRICS.